

Frame to Frame Diffeomorphic Motion Analysis from Echocardiographic Sequences

Zhijun Zhang, David Sahn, Xubo Song

► **To cite this version:**

Zhijun Zhang, David Sahn, Xubo Song. Frame to Frame Diffeomorphic Motion Analysis from Echocardiographic Sequences. Pennec, Xavier and Joshi, Sarang and Nielsen, Mads. Proceedings of the Third International Workshop on Mathematical Foundations of Computational Anatomy - Geometrical and Statistical Methods for Modelling Biological Shape Variability, Sep 2011, Toronto, Canada. pp.15-24, 2011. <inria-00623833>

HAL Id: inria-00623833

<https://hal.inria.fr/inria-00623833>

Submitted on 15 Sep 2011

HAL is a multi-disciplinary open access archive for the deposit and dissemination of scientific research documents, whether they are published or not. The documents may come from teaching and research institutions in France or abroad, or from public or private research centers.

L'archive ouverte pluridisciplinaire **HAL**, est destinée au dépôt et à la diffusion de documents scientifiques de niveau recherche, publiés ou non, émanant des établissements d'enseignement et de recherche français ou étrangers, des laboratoires publics ou privés.

Frame to Frame Diffeomorphic Motion Analysis from Echocardiographic Sequences

Zhijun Zhang¹, David J. Sahn^{1,2}, and Xubo Song¹

¹ Department of Biomedical Engineering

² Department of Pediatric Cardiology

Oregon Health and Science University

20000 NW Walker Road, Beaverton, OR 97006, USA

{zhangzhi, songx, sahn}@ohsu.edu

Abstract. Quantitative motion analysis from echocardiography is an important yet challenging problem. We develop a motion estimation algorithm for echocardiographic image sequences based on diffeomorphic image registration in which the velocity field is spatiotemporally smooth. The novelty of this work is that instead of optimizing a functional of velocity field which consists of similarity metrics between a reference image to each of the following images (*first-to-follow*), we optimize a functional which is a sum of similarity metrics of each two consecutive images (*frame-to-frame*). This method can reduce the bias effect of using a single image as reference. It also improves registration accuracy since consecutive frames usually have higher dependency than frames far away. We validate our method by using both simulated images with known ground truth and *in vivo* pig heart images with sonomicrometry. Tests indicate that our frame-to-frame motion estimation method is more accurate than first-to-follow method.

1 Introduction

Quantitative analysis of cardiac deformation and motion is important for studying heart function. Many illnesses related to ischemia or infarct can be recognized from the motion and deformation abnormalities [1]. Techniques to discriminate the abnormal motion and accurately locate regions with motion abnormality are critical to identify the disease and to evaluate the treatment. Echocardiography (echo) is the most widely used image modality because it is non-ionizing, real-time, cost-effective and convenient. With the development of the new transducer array technology, 3D echo can now provide real-time images of the whole heart [2]. However, due to the low signal-noise-ratio, general methods for motion estimation do not work well on echo images. In addition, the 4D (3D+t) data is acquired with a compromise that both the spatial and temporal resolutions are reduced comparing to 2D+t sequences. As a result, 3D motion analysis from echo sequences remains a challenging problem.

Cardiac motion analysis algorithms can be classified into three categories: model-based, feature-based and voxel-based methods. Lots of cardiac models

have been proposed for motion analysis and segmentations [3]. Surface models such as super-quadrics are used for motion analysis by fitting the model with a sequence of images [4, 5], however, these models only estimate the deformation on the model surfaces. Comaniciu *et al.* [6] proposed a Kalman filter based shape tracking method by using information fusion framework with a probabilistic subspace model constraint. In this work, a shape model needs to be learned and the motion estimation is limited along the contour points. Volumetric models such as dynamic finite elements have been used to estimate the deformation inside the myocardium [7, 8]. Wang *et al.* [9] tracked myocardial surface points by maximizing the likelihood of a combined surface and a two-steps motion prediction model. Both the initial myocardial surface detector and the motion prediction model need to be learned in advance. Generally speaking, deformable model based methods needs prior knowledge related to the models and their generation needs some sort of human interaction. Feature-based methods use landmarks such as the tagged lines to fit the deformable model such as 4D B-spline [10]. However, in echocardiography due to lack of stable landmarks in the myocardium and artificial features such as the tagged line are not available, feature-based method is difficult to estimate the deformation by using trustable correspondence. Voxel-based methods require no manual intervention, they estimate spatially dense transformations from all image voxels directly. This method can be implemented as an automatic method and we focus our work on this approach. Voxel based image registration methods such as optical-flow [11] and B-spline based methods [12, 13] have been proposed for cardiac motion analysis from echo images. However, the motion analysis problem is simplified into a series of independent pairwise image registrations and the temporal motion smoothness is not considered. To enforce the temporal consistency of particle motion, many temporal models have been used. Carbayo *et al.* [14] proposed a spatiotemporal deformation model for cardiac motion tracking. A 2D+t B-spline transformation with spatiotemporal smoothness is used with the first frame as the reference. A 3D+t extension is proposed by Metz *et al.* [15] and the average image is used as the reference. Particle trajectory constraint such as polynomial modeling has been used to regularize the spatiotemporal motion smoothness [16]. Diffeomorphic image registration is a method which the transformation is implicitly spatiotemporally smooth. The transformation between two images is defined as the end point of a velocity field flow which will be obtained by optimization of an energy functional of it. It has a very useful characteristic in computational anatomy that the transformation is one-to-one mapping and topology preserving [17]. This large deformation topology preserving property is preferred in cardiac motion analysis because of the fact that the deformation from the reference frame (usually the end of diastolic) to the mostly contracted frame (the end of systolic) is so large that deformation models without topology preserving constraint may cause the transformation to fold over or tear apart, which is not physically plausible. Beg *et al.* [18] proposed a large deformation diffeomorphic metric mapping algorithm (LDDMM) in which the smooth velocity field is estimated by optimizing a sum of squared difference (SSD) energy.

Khan *et al.* [19] extended the LDDMM method to analyze the anatomical shape evolution in an image sequence. De Craene *et al.* [20] proposed a method in which the velocity field is defined as temporal piecewise continuous 3D B-spline functions and the B-spline control parameters are estimated by optimization of a parameterized energy function. In a following work [21], the velocity field is defined as a 3D+t spatiotemporal B-spline model to reduce B-spline control points in temporal direction. In both methods, the optimal velocity field minimizes the summed dissimilarity metrics between the first frame and each of the unwarped subsequent frames, which we call them *first-to-follow* methods. It has been presented theoretically and experimentally that speckle pattern will change under large deformation [22] and that registration of frames further away from the reference is less accurate due to speckle de-correlation [12]. We propose a diffeomorphic registration method with a spatiotemporally smooth velocity field which minimizes the summed SSDs of the unwarped consecutive frames (*frame-to-frame* method). Our registration method is tested with simulated and *in-vivo* pig datasets, the results show that the accuracy is improved over first-to-follow method.

2 Method

2.1 Diffeomorphic Image Sequence Registration

A diffeomorphism flow is a dynamic system with each of the diffeomorphism to be a state in a differentiable manifold [23]. We define a flow $\phi(\mathbf{x}, t), t \in [0, T], \mathbf{x} \in \Omega \subset R^d (d = 2, 3)$ with its smooth velocity field $\mathbf{v}(\mathbf{x}, t)$ by using the differential equation of $\frac{d\phi}{dt} = \mathbf{v}(\phi(\mathbf{x}, t), t)$. It has been proven in [24] that if $\mathbf{v}(\mathbf{x}, t)$ is smooth enough with a differential operator L in a Sobolev space V , then the transformation $\phi(\mathbf{x}, t)$ will be a group of diffeomorphisms with t varying from 0 to T . The diffeomorphic image registration is stated as a variational problem, that given two images I_0 and I_1 , to find an optimal velocity field $\hat{\mathbf{v}}$ which minimizes an energy functional consisting of a sum of squared difference (SSD) and a geodesic distance metric between $\phi(\mathbf{x}, 0)$ and $\phi(\mathbf{x}, T)$ [18]:

$$\hat{\mathbf{v}} = \arg \inf_{\mathbf{v} \in V} \lambda \int_0^T \|\mathbf{v}(\mathbf{x}, t)\|_V^2 dt + \int (I_0(\mathbf{x}) - I_1(\phi(\mathbf{x}, T)))^2 d\mathbf{x}, \quad (1)$$

with λ being the weight to balance these two energies. If we have a sequence of N_f images to be registered, the similarity metric consists of the SSD of the difference between a reference frame I_0 and each of the deformed subsequent frames $I_k(\phi(\mathbf{x}, t_k)), k = 1, 2, \dots, N_f$. Then the mathematical form can be in a similar form as [19]:

$$\hat{\mathbf{v}} = \arg \inf_{\mathbf{v} \in V} \lambda \int_0^T \|\mathbf{v}(\mathbf{x}, t)\|_V^2 dt + \sum_{k=1}^{k=N_f} \int (I_0(\mathbf{x}) - I_k(\phi(\mathbf{x}, t_k)))^2 d\mathbf{x}. \quad (2)$$

This scheme has two disadvantages: first, the speckle de-correlation between far away frames are high which may cause correspondence ambiguity between

the two images; second, it takes longer time to converge since the difference between reference frame to far away frames is bigger than that of the consecutive frames. Instead of optimizing each deformed subsequent frames to be similar to the reference frame, we propose a variational energy which minimizes the difference between every two deformed consecutive frames $I_{k-1}(\phi(\mathbf{x}, t_{k-1}))$ and $I_k(\phi(\mathbf{x}, t_k))$:

$$\hat{\mathbf{v}} = \arg \inf_{\mathbf{v} \in V} \lambda \int_0^T \|\mathbf{v}(\mathbf{x}, t)\|_V^2 dt + \sum_{k=1}^{k=N_f} \int (I_{k-1}(\phi(\mathbf{x}, t_{k-1})) - I_k(\phi(\mathbf{x}, t_k)))^2 d\mathbf{x}, \quad (3)$$

we denote the two energy terms in Eqn.(3) as E_{reg} and E_{ssd} respectively. This method will find a flow of diffeomorphisms which have the shortest geodesic path in the manifold and simultaneously minimizes summed errors of each two neighboring images. This will improve the accuracy of the transformation since the neighboring frames generally have higher intensity correlation than those which are not neighbors. It can also reduce the chance that the transformation is biased due to noise in the reference images. Our frame-to-frame method is different from the method which simply estimates the diffeomorphisms between consecutive frames and then composites together. In our method, minimizing the difference between two consecutive frames jointly optimizes all the velocity field before and between the time of these two frames.

The direct solution for this variational framework is expensive. Alternatively, a parameterized representation of the velocity field is used [25], where the velocity field is represented as a series of B-spline functions and the displacement field can be expressed as the forward Euler integral of velocity field. We use a spatiotemporally smooth B-spline function to represent the velocity field. It is defined as $\mathbf{v}(\mathbf{x}, t_k) = \sum \mathbf{c}_{i;k} \boldsymbol{\beta}(\mathbf{x} - \mathbf{x}_i)$, with $\mathbf{c}_{i;k}$ being the B-spline control vectors at t_k located on a uniform grid of \mathbf{x}_i , $\boldsymbol{\beta}(\mathbf{x} - \mathbf{x}_i)$ is the 3D B-spline kernel function which is the tensor product of the 1-D B-spline functions. Define $\phi_k = \phi(\mathbf{x}, t_k)$ the transformation at time step t_k , we assume the velocity is piecewise constant within a time step, then we have $\phi_k = \phi_{k-1} + \mathbf{v}(\phi_{k-1}, t_{k-1}) \Delta t$, with $\phi_0(\mathbf{x}) = \mathbf{x}$, $k = 1, 2, \dots, N_t$, with N_t being the total number of time steps of the velocity field. Without loss of generality, we can have $\Delta t = 1$. In our test, we use one time step in velocity field between two neighboring frames since the deformation between them is usually small, that is $N_t = N_f$. However, our method easily generalizes to multiple time steps between frames if the deformation between two consecutive frames is large. The energy functional will be a parameterized function of $\mathbf{c}_{i;k}$ and it can be optimized by using a steepest descent method.

2.2 Regularization

In order to assure the $\phi(\mathbf{x}, t)$ to be diffeomorphic, we need to define $\mathbf{v}(\mathbf{x}, t)$ to be spatiotemporally smooth under a differential operator L . The linear operator we choose is: $L = \nabla^2 \mathbf{v} + w_t \frac{d\mathbf{v}}{dt}$, with $\nabla^2(\cdot)$ being a Laplacian operator and w_t a

constant weight. In the discrete time form of velocity field, the time integral of the norm in V space of Eqn.(3) will be: $E_{reg} = \sum_{k=1}^{N_t} \sum_{\mathbf{x}} (\nabla^2 \mathbf{v}_k)^2 + w_t \sum_{k=2}^{N_t} \sum_{\mathbf{x}} |\mathbf{v}_k(\mathbf{x} + \mathbf{v}_{k-1} \Delta t) - \mathbf{v}_{k-1}|^2$, with $\mathbf{v}_k = \mathbf{v}(\mathbf{x}, k)$. The first term makes the velocity field spatially smooth which is denoted as E_{sr} . The second term keeps the particle velocity smooth and it is denoted as E_{tr} . The overall effect is to keep the velocity field spatiotemporally smooth.

2.3 Optimization

We use a steepest descent method to optimize the parameterized function. The derivative of the total registration energy with respect to the transformation parameters will be calculated analytically. The derivative of the similarity metric with respect to the B-spline parameters $\mathbf{c}_{i;k'}$ is:

$$\frac{\partial E_{ssd}}{\partial \mathbf{c}_{i;k'}} = \sum_{k=1}^{N_f} (I_k(\phi_k) - I_{k+1}(\phi_{k+1})) (\nabla I_k(\phi_k) \frac{\partial \phi_k}{\partial \mathbf{c}_{i;k'}} - \nabla I_{k+1}(\phi_{k+1}) \frac{\partial \phi_{k+1}}{\partial \mathbf{c}_{i;k'}}), \quad (4)$$

with $\frac{\partial \phi_k}{\partial \mathbf{c}_{i;k'}}$ being the Jacobian matrix of transformation at time step k with respect to the i th B-spline coefficient in k' th frame. It can be calculated with chain rule and it is zero when $k' \geq k$. For detailed computation refer to [21].

For the derivative of the spatial and temporal regularization energies with respect to the m th component of $\mathbf{c}_{i;k}$, we have:

$$\frac{\partial E_{sr}}{\partial c_{i,m;k}} = \sum_{\mathbf{x} \in \Omega'} \beta_m''(\mathbf{x} - \mathbf{x}_i), \quad (5)$$

with Ω' being the local support of the B-spline kernel function, and $\beta_m''(\cdot)$ being the second derivative of the B-spline function with respect to m th component. Considering that the displacement between two time step is small, we have:

$$\frac{\partial E_{tr}}{\partial c_{i,m;k}} \approx w_t \sum_{\mathbf{x} \in \Omega'} (2 * v_{i,m;k} - v_{i,m;k-1} - v_{i,m;k+1}) \beta(\mathbf{x} - \mathbf{x}_i). \quad (6)$$

The registration energy can be optimized by starting from initial position and descending along the negative gradient direction at each iteration until there is no significant decrease.

2.4 Implementation

In our implementation, we use a series of B-spline transformations with grid spacing of 10 in each dimension to represent the velocity field. The values of λ and w_t are set to be 0.1 and 0.5. The algorithm is implemented with Matlab under a windows XP 64 bit system on a machine with 2.13GHz Xeon 8 cores CPU and 6GB memory. It takes about 1 hour to register a 3D (3 minutes for a 2D) sequence with 20 frames.

3 Experiment and Data

We use both simulated and real data to validate our algorithm. In the simulated data experiment, a longitudinal view of a diastolic left ventricle (LV) image with size of 274×192 is used as the reference image. This frame is then deformed with a series of continuous displacement field functions. The deformations are symmetrical along the long axis of the LV to simulate the myocardial contraction effect along radial and longitudinal directions. The displacement functions are in form of: $f_x(i) = a_x \sin \frac{\pi(x-x_c)}{2r_d} \sin(\frac{i\pi}{N_f})$ and $f_y(i) = a_y \sin \frac{\pi(y-y_{apex})}{2(y_{base}-y_{apex})} (\sin(\frac{i\pi}{N_f} + \frac{\pi}{16}) - \sin \frac{\pi}{16})$, with x_c, r_d the axis center coordinate and the average axial radius of LV, y_{apex} and y_{base} the height of base and apex planes, N_f and i the number of frames and the frame index, and a_x, a_y are the magnitudes of displacement fields. An image sequence with $N_f + 1$ frames is generated when i varies from 0 to N_f to simulate the cardiac motion in one cycle.

We carry out two experiments for the simulated data. In the first experiment, three sequences with 20 frames each are simulated with multiplicative speckle noise of variance 0.06, 0.08 and 0.10 added. The reference frame and the 10th frame with speckle noise variance 0.10 are shown together with the ground truth displacement field in Fig.1. In the second simulated experiment, we first generate 20 frames without deformation by adding independent speckle noise of variance 0.10 to the reference frame. Then each of the frame I_i will have a percentage p pixels replaced with the intensity at the same position in frame I_{i-1} . By updating noisy image one by one we assure that the two consecutive frames to have noise overlap ratio of p . Each frames will then be deformed by using the ground truth displacement fields. We simulate two sequences with overlap ratio of 0.2 and 0.4 respectively.

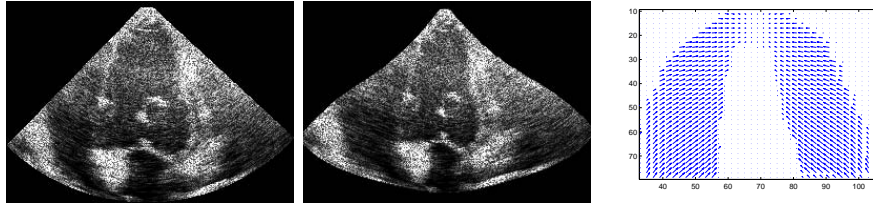


Fig. 1. The reference frame and the 10th frame in speckle variance 0.1 test and the displacement field (only displacement field inside a bell-shaped mask is displayed).

A real world dataset is acquired from an open-chest pig by using a Philips IE33 system. For validation, we installed six sonomicrometers in the heart wall. The distances between each pair of the sonomicrometers are recorded with the image sequences and are used as ground truth to compare with the tracked distance in the echo images. The images are resampled into volume sequences of $160 \times 100 \times 128$ with voxel size $1mm \times 1mm \times 1mm$. The crystal coordinates in the reference frame are manually denoted.

4 Result

In the first simulated experiment, we compare our frame-to-frame method with the first-to-follow method by tracking the trajectories of the points in the myocardial wall during the motion process. The estimated trajectories of four example points from a small region of the myocardium for speckle noise variance 0.06 test are shown in Fig.2, where the ground truth trajectories are overlaid for comparison. We can see generally coordinates of the points in each time step in our method are closer to the ground truth position than the first-to-follow method.

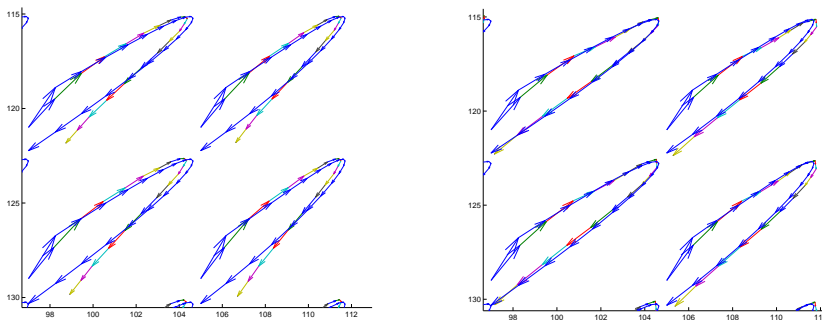


Fig. 2. Points trajectories in the first-to-follow method (left) and the frame-to-frame method (right). The ground truth trajectories (blue) are overlaid with the estimated curves (multiple color) for comparison. The arrow shows the velocity at each time step.

In Fig.3 we illustrate the motion estimation errors in both x and y coordinates in noise level 0.08 dataset. We can see that the motion estimation errors of x and y coordinates in most of frames in our method are closer to zero than those of the first-to-follow method. The figure also shows that our method has a smaller error variance in both coordinates. The mean of magnitude of errors in the three noise variance levels in frame-to-frame method are 0.23, 0.26 and 0.32, while in first-to-follow method they are 0.38, 0.45 and 0.56 respectively.

In the second test, the motion estimation errors in y coordinates for two methods are shown in Fig.4. The results are similar for x coordinate errors. We can see the results of frame-to-frame method are better than those in first-to-follow method in means and standard deviations of errors. We can see for the frame-to-frame method, when the intensity correlation between two images is increased, the mean and variance of the registration error are decreased. In the results of first-to-follow methods, the error mean does not change obviously when the correlation between consecutive frames are increased.

In the *in-vivo* open-chest pig test, we compare the performance of the two algorithms by computing the correlations over time between the algorithm-derived pair-wise distances with sonomicrometry, shown in Table.1. Sonomicrometry pro-

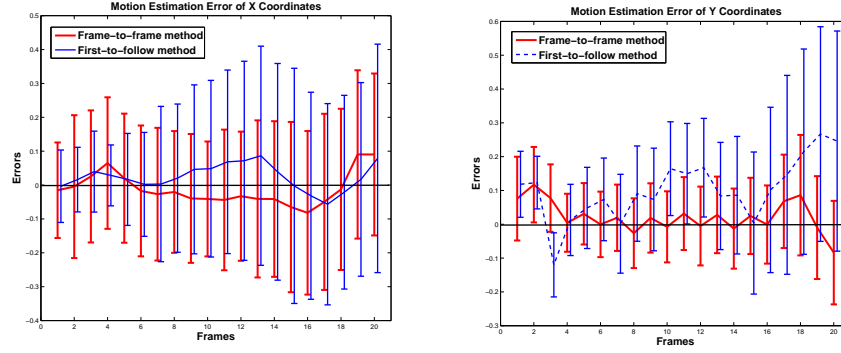


Fig. 3. The motion estimation errors in x (left) and y (right) coordinates of frame-to-frame method and first-to-follow method. The error bars shows the standard deviation of the errors in each frames. The horizontal lines represent the curves of zero mean transformation errors to help comparison.

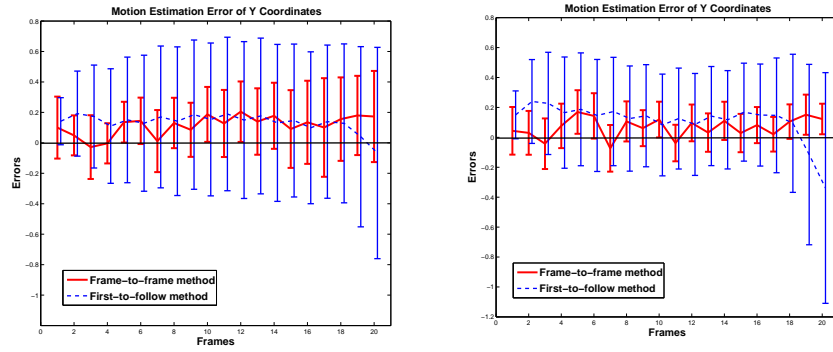


Fig. 4. The motion estimation errors in y coordinates of frame-to-frame method and first-to-follow method. The left and right figures show the results of 20 and 40 percent noise overlap tests. The horizontal lines show the zeros mean transformation errors.

vide the ground truth distances between each two of the crystals. We can clearly see the improvement of our proposed method.

Table 1. The correlations between the estimated pair-wise distances and those from the sonomicrometry, with frame-to-frame method (numbers to the left) and the first-to-follow method (numbers to the right). Numbers 1-6 index the six sonomicrometry markers.

	1	2	3	4	5	6
1	1.0/1.0	0.936/0.907	0.901/0.885	0.913/0.902	0.948/0.923	0.859/0.831
2	0.936/0.907	1.0/1.0	0.881/0.856	0.927/0.904	0.887/0.838	0.951/0.916
3	0.901/0.885	0.881/0.856	1.0/1.0	0.825/0.786	0.902/0.905	0.819/0.788
4	0.913/0.902	0.927/0.904	0.825/0.786	1.0/1.0	0.937/0.919	0.934/0.902
5	0.948/0.923	0.887/0.838	0.902/0.905	0.937/0.919	1.0/1.0	0.918/0.873
6	0.859/0.831	0.951/0.916	0.819/0.788	0.934/0.902	0.918/0.873	1.0/1.0

5 Conclusion

We propose a large deformation diffeomorphic registration method by minimizing the difference between every *consecutive images*. Simulation test shows that our frame-to-frame method has a higher estimation accuracy of motion than the first-to-follow method. Validation with sonomicrometry also shows that our motion estimation result has higher consistency with real data.

Acknowledgement

This paper is supported by a NIH/NHLBI grant 1R01HL102407-01 awarded to Xubo Song and David Sahn.

References

1. Fukuda, K., Oki, T., Tabata, T., Iuchi, A., Ito, S.: Regional left ventricular wall motion abnormalities in myocardial infarction and mitral annular descent velocities studied with pulsed tissue Doppler imaging. *JASE*, 11(9), 841–848 (1998)
2. Hung, J., Lang, R., Flachskampf, F., Shernan, S.K., McCulloch, M.L., Adams, D.B., Thomas, J., Vannan, M., Ryan, T.: 3D Echocardiography: A Review of the Current Status and Future Directions. *JASE*, 20(3), 213–233 (2007)
3. A.F. Frangi, W.J. Niessen, and Max A. Viergever. “Three-Dimensional Modeling for Functional Analysis of Cardiac Images: A Review.” *IEEE Trans. Med. Imaging*, vol.20, no.1, pp.1–25, 2001.
4. Eric Bardinet, Laurent D. Cohen and Nicholas Ayache. “Tracking and motion analysis of the left ventricle with deformable superquadrics. *Medical Image analysis*, vol.1, no.2, pp:129–149, 1996.
5. Jinah Park, Dimitri Metaxas, Alistair A. Young and Leon Axel. “Deformable Models with Parameter Functions for Cardiac Motion Analysis from Tagged MRI Data.” *IEEE Transactions on Medical Imaging*, vol.15, no.3, pp.278–289, June, 1996.
6. Comaniciu, D, Zhou, X., Krishnan, S.: Robust tracking of myocardial border: An information fusion approach. *IEEE Trans. Med. Imag.* 23(7), 849–860 (2004)

7. Papademetris, X., Sinusas, A.J., Dione, D.P., Duncan, J.S.: Estimation of 3D left ventricular deformation from echocardiography. *Med. Imag. Anal.* 5(1), 17–28 (2001)
8. Joel Schaerera, Christopher Casta, Jerome Pousina and Patrick Claryssea. “A dynamic elastic model for segmentation and tracking of the heart in MR image sequences.” *Medical Image Analysis*, vol.14, pp.738–749, 2010.
9. Wang, Y., Georgescu, B., Houle, H., Comaniciu, D.: Volumetric Myocardial Mechanics from 3D+t Ultrasound Data with Multi-model Tracking. In *STACOM 2010*. LNCS vol. 6364, 184–193. Springer, Heidelberg (2010)
10. J. Huang, D. Abendschein, V. Davila, A.A. Amini, “Four-dimensional LV tissue tracking from tagged MRI with a 4D B-spline model.” *IEEE Trans Medical Imaging*, vol.18, no.10, 1999.
11. Suhling, M., Arigovindan, M., Jansen, C., Hunziker, P., Unser, M.: Myocardial Motion Analysis from B-Mode Echocardiograms. *IEEE Trans. Image Process.*, 14(4) 525–536 (2005)
12. Elen, A., Choi, H.F., Loeckx, D., Gaom, H., Claus, P., Suetens, P., Maes, F., D’hooge, J.: Three-dimensional cardiac strain estimation using spatio-temporal elastic registration of ultrasound images: a feasibility study. *IEEE Trans. Med. Imag.*, 27(11), 1580–1591, (2008)
13. Myronenko, A., Song, X.B., David, J.S: LV Motion Tracking from 3D Echocardiography Using Textural and Structural Information. *MICCAI 2007*. 428–435 (2007)
14. Ledesma-Carbayo, M.J., Mah-Casado, P., Santos, A., Prez-David, E., GarMA, Desco, M.: Spatio-Temporal Nonrigid Registration for Ultrasound Cardiac Motion Estimation. *IEEE Trans. Med. Imag.*, 24(9), 1113–1126 (2005)
15. Metz, C.T., Klein, S., Schaap, M., Walsum, T., Niessen, W.J.: Nonrigid registration of dynamic medical imaging data using nD+t B-splines and a groupwise optimization approach. *Med. Imag. Anal.* 15(2), 238–249 (2011)
16. Castillo, E., Castillo, R., Martinez, J., Shenoy, M., Guerrero, T.: Four-dimensional deformable image registration using trajectory modeling. *Physics in Medicine and Biology*, 55, 305–327 (2010)
17. Miller, M.I; Computational anatomy: shape, growth, and atrophy comparison via diffeomorphisms. *Neuroimage*, 23(1), 19–33 (2004)
18. Beg, M.F.; Miller, M.I.; Troune, A.; Younes, L.; Computing Large Deformation Metric Mappings via Geodesic Flows of Diffeomorphisms. *INT J COMPUT VISION*. 61(2), 139–157 (2005)
19. Khan, A.R.; Beg, M.F.; Representation of time-varying shapes in the large deformation diffeomorphic framework. *ISBI 2008*, 1521–1524 (2008)
20. Craene, M.; Camara, O.; Bijnens, B.H.; Frangi, A.F.: Large Diffeomorphic FFD Registration for Motion and Strain Quantification from 3D-US Sequences, *Functional Imaging and Modeling of the Heart, FIMH’09*, LNCS vol.5528, 437–446 (2009)
21. Craene, M.; Piella, G.; Duchateau, N.; Silva, E.; Doltra, A.; Gao, H.; D’hooge, J.; Camara, O.; Brugada, J.; Marta Sitges: Temporal Diffeomorphic Free-Form Deformation for Strain Quantification in 3D-US Images. *MICCAI 2010*, 1–8 (2010)
22. Meunier, J.: Tissue motion assessment from 3D echographic speckle tracking. *Phys. Med. Biol.* 43, 1241–1254 (1998)
23. Arrowsmith, D.K.; Place, C. M.: An introduction to dynamical systems. Cambridge Press, UK (1990)
24. Dupuis, P.; Grenander, U.: Variational problems on flows of diffeomorphisms for image matching. *Q APPL MATH.* 56(3) 587–600 (1998)
25. Ashburner, J.; A fast diffeomorphic image registration algorithm. *NeuroImage*, 38(1), 95–113 (2007)